COMPUTER METHODS AND PROGRAMS IN BIOMEDICINE 110 (2013) 389–398

journal homepage: www.intl.elsevierhealth.com/journals/cmpb

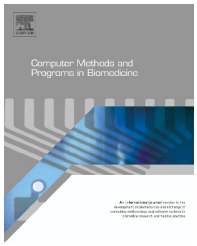

An FDTD-based computer simulation platform for shock wave propagation in electrohydraulic lithotripsy

Bülent Yılmaz[a,*], *Emre Çiftçi*[b]

[a] *Abdullah Gül University, Biomedical Engineering Department, Kayseri, Turkey*
[b] *Başkent University, Biomedical Engineering Department, Ankara, Turkey*

ARTICLE INFO

Article history:
Received 20 September 2012
Received in revised form
26 November 2012
Accepted 28 November 2012

Keywords:
Finite-difference time-domain method
Lithotripsy
Shock wave
Computer simulation

ABSTRACT

Extracorporeal Shock Wave Lithotripsy (ESWL) is based on disintegration of the kidney stone by delivering high-energy shock waves that are created outside the body and transmitted through the skin and body tissues. Nowadays high-energy shock waves are also used in orthopedic operations and investigated to be used in the treatment of myocardial infarction and cancer. Because of these new application areas novel lithotriptor designs are needed for different kinds of treatment strategies. In this study our aim was to develop a versatile computer simulation environment which would give the device designers working on various medical applications that use shock wave principle a substantial amount of flexibility while testing the effects of new parameters such as reflector size, material properties of the medium, water temperature, and different clinical scenarios. For this purpose, we created a finite-difference time-domain (FDTD)-based computational model in which most of the physical system parameters were defined as an input and/or as a variable in the simulations. We constructed a realistic computational model of a commercial electrohydraulic lithotriptor and optimized our simulation program using the results that were obtained by the manufacturer in an experimental setup. We, then, compared the simulation results with the results from an experimental setup in which oxygen level in water was varied. Finally, we studied the effects of changing the input parameters like ellipsoid size and material, temperature change in the wave propagation media, and shock wave source point misalignment. The simulation results were consistent with the experimental results and expected effects of variation in physical parameters of the system. The results of this study encourage further investigation and provide adequate evidence that the numerical modeling of a shock wave therapy system is feasible and can provide a practical means to test novel ideas in new device design procedures.

1. Introduction

A shock wave is an acoustical wave with high-intensity peak pressure. Since 1980, shock waves have been used in the treatment of different types of health problems. The pioneering application of the shock waves used in the medical field is the Extracorporeal Shock Wave Lithotripsy (ESWL) system. ESWL is based on disintegration of the stone so that they can easily pass through the urinary tract by delivering high-energy shock waves that are created outside the body through the skin and body tissues until they hit the denser kidney

* *Corresponding author*. Tel.: +90 352 224 8800; fax: +90 352 338 8828.
E-mail addresses: bulent.yilmaz@agu.edu.tr (B. Yılmaz), emrecif@gmail.com (E. Çiftçi).
0169-2607/$ – see front matter
http://dx.doi.org/10.1016/j.cmpb.2012.11.011

stones. This is the most common therapeutic approach used in patients with relatively large diameter kidney stones. There are three types of ESWL systems; electromagnetic, electrohydraulic, and piezoelectric lithotriptors. Electromagnetic and electrohydraulic lithotriptors dominate the lithotripsy market today.

Extracorporeal shock waves are also employed in the treatment of musculo-skeletal conditions such as plantar heel spurs [1], plantar fasciitis [2] and tennis elbow [3]. Recently, results from several investigational studies have shown that extracorporeal shock waves could be used in the treatment of myocardial infarction [4,5] and cancer [6]. In these applications shock waves have been shown to trigger the body's own natural repair mechanisms and stimulate healing.

In order to enable the development of devices designed for the treatment of various diseases, it is necessary to estimate the associated field parameters. For this purpose, different applications require modeling and analysis of acoustical wave propagation. There are mainly two approaches in accurate modeling of a specific problem: analytical and numerical methods. Analytical modeling approaches seek solutions to the problem using analytical equations to represent the media and physical processes. However, this approach can be utilized only in simplified geometric models. On the other hand, numerical methods aim to solve the problem by discretizing the associated media and differential equations. Finite-difference time-domain (FDTD) method is a popular numerical modeling technique. In the application of electrodynamics problems time-dependent Maxwell's equations in partial differential form are discretized using central-difference approximations to the space and time partial derivatives. The resulting finite-difference equations are solved iteratively in such a manner that the electric field vector components in a volume of space are solved at a given instant in time; then the magnetic field vector components in the same spatial volume are solved at the next instant in time; and the process is repeated over and over again until the desired transient or steady-state electromagnetic field behavior is fully evolved [7,8]. The system of equations used to represent the sound wave propagation is similar to that of electromagnetic waves, and thus, FDTD method can be applied in the computer simulations of propagation of sound waves. Pressure and velocity in sound wave correspond to electrical and magnetic fields in electromagnetic waves in the computations using FDTD method.

Although extracorporeal shock waves are now widely used in medical treatment, there are few examples of numerical modeling used in wave propagation analysis. Previously, Steiger [9] and Jian et al. [10] investigated computational modeling of electromagnetic lithotriptors. Steiger and Jian et al. used a commercial lithotriptor (Storz MODULITH SL 10) and Reichenberger's experimental setup [11], respectively, to validate their simulation results. These studies presented the measured and computed wave profiles in the acoustical focus in one dimension (pressure vs. time). In addition, Ukai et al. [12] developed a computational modeling scheme of shock waves used in osteotomy (cutting bones in a body without incising skin). They have developed a FDTD-based focused ultrasound propagation simulator for their setup.

In this current study our aim was to develop a versatile computer simulation environment which would give the device designers working on various medical applications that use shock wave principle a substantial amount of flexibility while testing the effects of new parameters such as reflector size, material properties of the medium, water temperature, and different clinical scenarios. For this purpose, we created an FDTD-based computational model in MATLAB (The MathWorks, Inc., Natick, MA, USA) in which most of the physical system parameters were defined as an input and/or as a variable in the simulations. This computer simulation environment makes it possible for the user to define the shock wave source characteristic, to select and adjust material and material properties used in the propagation media, location of the focal points, and to yield one (pressure vs. time at one point in space), two (pressure distribution in the *x*–*z* plane), and three (pressure distribution in the *x*–*y*–*z* volume, and pressure distribution in the *x*–*z* plane changing in time) dimensional pressure distribution graphs or movies. Different materials such as kidney, fat tissue, and bones, for which acoustical properties are available in the literature, may also be incorporated appropriately in the simulation environment.

In order to test this idea in a specific application, we constructed a realistic computational model of a commercial electrohydraulic lithotriptor (LithoDiamond, HealthTronics, Inc., TX, USA). We first optimized our simulation program using the results, such as maximum positive and minimum negative pressure levels in the proximity of the focal (F2) point location, that were obtained by the manufacturer in an experimental setup using hydrophone pressure sensors. This region is where we try to position the kidney stone in a lithotripsy system. Secondly, we compared the simulation results with an experimental setup in which oxygen level in water was varied. Finally, we studied the effects of changing the input parameters like ellipsoid size and material, temperature change in the wave propagation media, and shock wave source point misalignment.

2. Materials and methods

2.1. *Acoustic wave equation*

The acoustic wave equation governs the propagation of acoustic waves through a medium. The form of the equation is a second order partial differential equation. The equation describes the evolution of acoustic pressure p or particle velocity u as a function of space and time [13]:

$$K\frac{\partial}{\partial t}p(x,t) = \nabla u \tag{1}$$

$$K\frac{\partial}{\partial t}p(x,t) = \nabla u \rho_0 \rho_r \frac{d}{dt}u(x,t) = \nabla p(x,t) \tag{2}$$

where ρ_0 and ρ_r represent the density of water and the density of the material in the medium relative to water. K is the

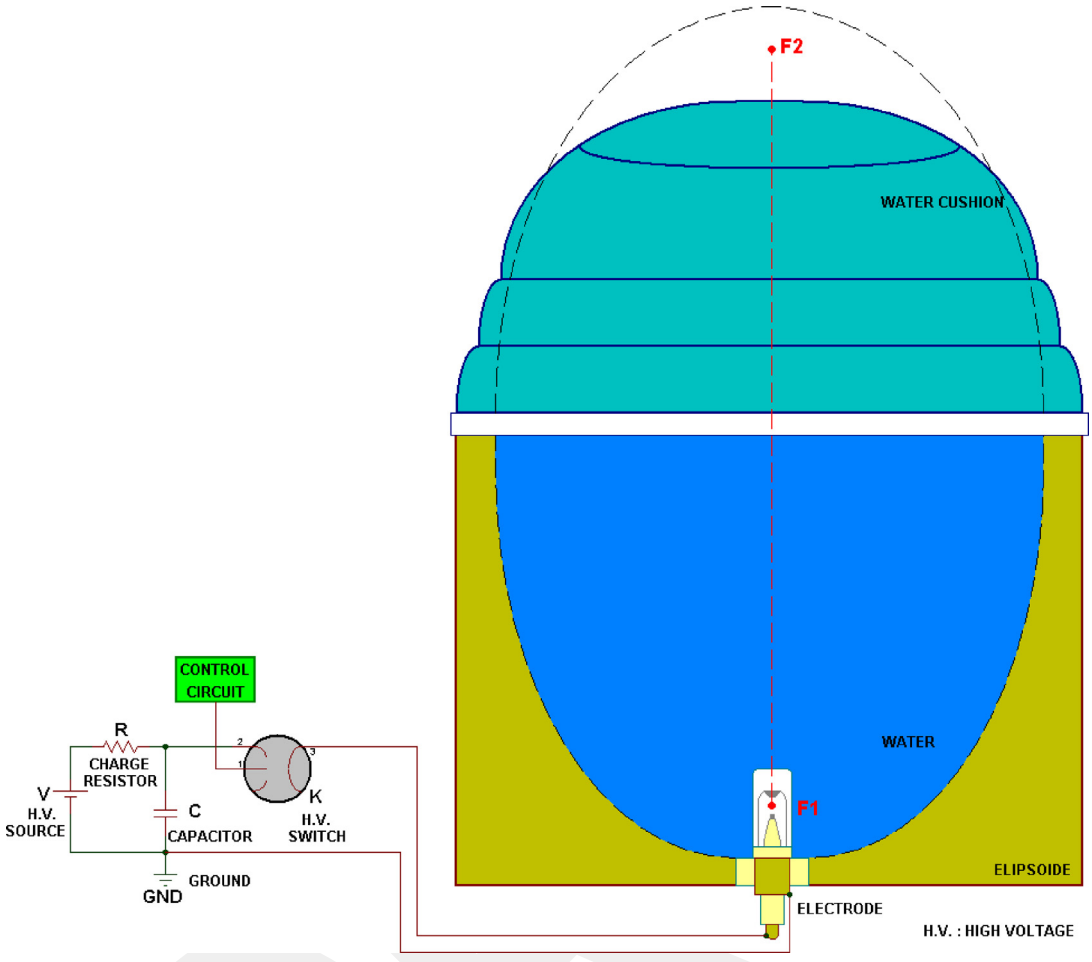

Fig. 1 – Graphical description of the realistic electrohydraulic lithotripsy system (LithoDiamond).

compressibility coefficient of the medium and the equation describing K is the following (c is the speed of sound):

$$K = \frac{1}{\rho \cdot c^2} = \frac{1}{\rho_0 \rho_r \cdot c^2} \tag{3}$$

2.2. *Numerical modeling using FDTD*

The numerical modeling of acoustical wave Eqs. (1) and (2) using FDTD is based on the discretization of these equations as described below. The equations are solved iteratively in such a manner that the pressure values in a volume of space are solved at a given instant in time; then the velocity values in the same spatial volume are solved at the next instant in time; and the process is repeated until the desired behavior is fully evolved.

For the iterative computation of these equations, realistic medium (ellipsoid reflector, water, air) properties have been assigned to each point in space according to the commercial lithotriptor (LithoDiamond) specifications provided by the manufacturer (see Fig. 1 for the graphical description of the electrohydraulic lithotripsy system).

Even though it is possible to define different shock wave source characteristics at the onset of the simulation (at F1 point), we used a discretized version of an analytical equation corresponding to the realistic pressure change in time in the shock wave employed in this commercial system. The analytical equation represent the discharge of a simple resistor–capacitor (RC) circuit, which is derived from the high voltage spark circuitry shown in Fig. 1. R, C (i.e., time constant τ) and charging voltage values are also defined as inputs to the simulation.

$$\frac{dp(x,y,z,t)}{dt} = \frac{1}{K(x,y,z)}\left[\frac{du_x(x,y,z,t)}{dx} + \frac{du_y(x,y,z,t)}{dy} + \frac{du_z(x,y,z,t)}{dz}\right] \tag{4}$$

$$\begin{aligned}\frac{p^{n+(1/2)}(i,j,k) - p^{n-(1/2)}(i,j,k)}{\Delta t} &= \frac{1}{k(i,j,k)}\left[\frac{u_x^n(i+(1/2),j,k) - u_x^n(i-(1/2),j,k)}{\Delta x}\right] \\ &+ \frac{1}{k(i,j,k)}\left[\frac{u_y^n(i,j+(1/2),k) - u_y^n(i,j-(1/2),k)}{\Delta y}\right] \\ &+ \frac{1}{k(i,j,k)}\left[\frac{u_z^n(i,j,k+(1/2)) - u_z^n(i,j,k-(1/2))}{\Delta z}\right]\end{aligned} \tag{5}$$

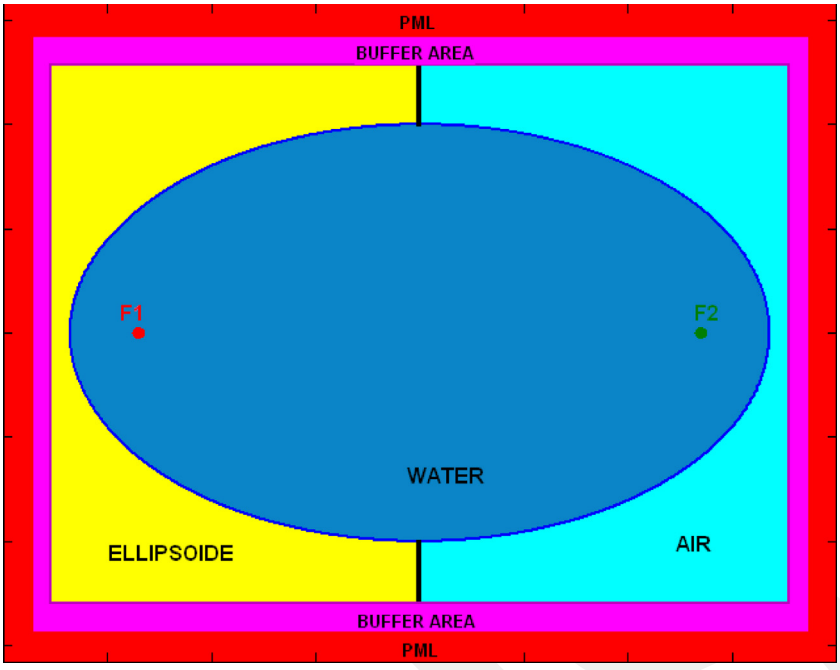

Fig. 2 – The central cross-section of the geometry used in the simulation (*x*–*z* plane). PML denotes Perfectly Matched Layer used as the absorbing boundary condition.

$$u_z^{n+(1/2)}\left(i,j,k+\frac{1}{2}\right) = u_z^{n-(1/2)}\left(i,j,k+\frac{1}{2}\right) + \frac{\Delta t}{\rho_r(i,j,k+(1/2))\cdot\rho_0\cdot\Delta z} \cdot[p^n(i,j,k+1)-p^n(i,j,k)] \quad (6)$$

$$ga(k) = \frac{\Delta t\cdot\rho_0\cdot\rho_r\cdot c^2}{\Delta z} \quad (7)$$

$$gb\left(k+\frac{1}{2}\right) = \frac{\Delta t}{\rho(k+(1/2))\cdot\rho_0\cdot\Delta z} \quad (8)$$

$$p^{n+(1/2)}(k) = p^{n-(1/2)}(k) + ga(k)\cdot\left[u_z^n\left(k+\frac{1}{2}\right) - u_z^n\left(k-\frac{1}{2}\right)\right] \quad (9)$$

$$u_z^{n+1}\left(k+\frac{1}{2}\right) = u_z^n\left(k+\frac{1}{2}\right) + gb\left(k+\frac{1}{2}\right) \cdot[p^{n+1/2}(k+1)-p^{n+1/2}(k)] \quad (10)$$

As seen in Fig. 2, in the geometry used for the computer simulations, half of the ellipsoid reflector was assigned as metal and a water cushion was placed in the second half. Water cushion was filled with water, and was surrounded by air. In different simulations different parameters were assigned to these media.

In FDTD method, the edge points in the simulation geometry are highly critical. When these points are not defined as wave pressure absorbing layers, the reflections substantially affect the simulation results. It becomes impossible to distinguish the actual reflections and the virtual reflections created due to these edge points. Thus, it is necessary to include absorbing boundary condition (ABC) in the simulation geometry. ABC can be defined quite differently in different applications. In this study, we adopted the "Perfectly Matched Layer" (PML) approach developed by Berenger [14] as an absorbing boundary condition to minimize reflections from the boundaries. In order to minimize the effect of PML on the ellipsoid boundary values an extra buffer layer was introduced between the PML and the ellipsoid geometry. The cell size of the area cannot be smaller than the "Perfectly Matched Layer (PML)". In PML every point is assigned an absorbing coefficient that decreases as the point is located further away from the edge points of the simulation geometry. If we select the buffer area size smaller than the PML size then the algorithm selects the coefficient points from both buffer layer and ellipsoid area. As a result of selecting different types of coefficient factor the simulation may calculate undesired reflections that can affect the simulation results. That is why we selected the buffer layer same size with the PML. The size of the buffer layer could be changed by the user and should at least be the size of PML.

Under normal conditions, when a shock wave is formed at the first focal point (F1) of the ellipsoid the highest pressure value occurs at the second focal point (F2). Because only half of the ellipsoid is used as the reflector, the location with the highest pressure moves to a more distant position on the same axis. Another important observation for the electrohydraulic lithotriptors is that the highest pressure does not occur in only one location rather it is distributed over an ellipsoidal

Table 1 – Input parameter list.

Parameter	Used value
Temperature	20 °C
Electrode resistance	580 kΩ
Capacitance	40 nF
Charge voltage	22 kV
Density of water	1000 kg/m^3
Density of brass	8400 kg/m^3
Density of air	1.2041 kg/m^3
Speed of sound (in water)	1482 m/s
Speed of sound (in brass)	343 m/s
Speed of sound (in air)	4700 m/s
Iteration time step size (Δt)	10 ns
Discretization spacing (Δz)	1 mm
Number of points in PML	10
Total simulation duration	24.85 μs

region which is referred to as the "zone of high pressure or focal zone".

2.3. *Optimization of simulation using experimental values*

In order to optimize our FDTD-based simulation we used experimental values obtained by the manufacturer of the commercial lithotriptor (LithoDiamond) using hydrophone pressure sensors (a special type of pressure transducer used in this field). For a set of system parameters listed in Table 1, the manufacturer provided us with the maximum positive (P^+ value 48.2 MPa) and minimum negative pressure (P^- value −6.8 MPa) values obtained in the focal zone. During the experiments it was also found that the distance between F2 point and the actual P^+ location was 4 mm in z-axis. In the simulation results, the computed pressure values were normalized to these experimental values.

2.4. *Visualization of simulation results*

Using the adjusted system parameters the simulations were executed and the pressure values changing in time and space were stored. The execution duration was 18 min for a Laptop PC with 2 GHz dual core processor and 2 GB RAM. We also developed a supporting code for the visualization of simulation results in one, two, and three dimensions (1D, 2D, 3D). The pressure distribution along the focal points axis (1D), focal points axis cross-section, *x*–*z* axis (2D), focal zone volume (3D), and time changing pressure values at the maximum pressure point (1D) are the options for the visual analysis of the results. For the spatial distribution graphs, red and blue represent positive and negative pressure values, respectively.

2.5. *Tests for simulations*

The tests we used to investigate the performance of our simulation environment can be grouped into two categories. The first test category included the comparison of simulation results with the results from an experimental setup obtained by the manufacturer to test the performance of their device when the gas amount in water was changed. The experimental setup is shown in Fig. 3. In that setup they placed a test stone at the F2 location of the lithotriptor and analyzed the number of shocks to totally disintegrate the stone when the gas amount in water was 2.5 mg/L and 1.5 mg/L. Decreasing the gas amount in water was achieved by reducing the dissolved oxygen amount in water. It is also known that the composition and behavior of cavitation bubbles (another important factor thought to play a role in the disintegration of the stones) is dependent on the pressures of gases dissolved in the fluid, the ambient pressure of the fluid, the vapor pressure of the fluid, and the diffusion velocities of the dissolved gases. In this test we did not take the effects of these into account and we simply observed the pressure distribution occurring in the focal zone when the gas amount was decreased 1 mg/L. For this purpose we decreased the water density parameter from 1000 kg/m^3 to 900 kg/m^3.

The second category included a series of tests investigating the effects of changes in various parameters to the performance of the lithotripsy system. The parameters we studied were the following: (1) temperature of the water and air was increased from 0 to 30 °C, (2) reflector material (brass) was replaced with aluminum, (3) outer medium (air) was replaced with water, (4) ellipsoid dimensions were reduced, and (5) location of the electrode used for the shock wave generation is shifted 5 mm toward right of the F1 point.

First of all, in order to apply the temperature increase in water and air, we increased the speed of sound in these media and decreased the density of air from 1.292 kg/m^3 to 1.165 kg/m^3. The speed of sound in water was increased from 1402 to 1507 m/s and speed of sound in air was increased from 331 to 349 m/s. These values were obtained from the literature. Patient comfort has always been the main concern for a water temperature level adjustment; however, it has never been addressed as a performance criterion up to now.

Secondly, when the brass reflector was replaced with an aluminum reflector the density of the reflector material was decreased from 8400 to 2560 kg/m^3. In most of the electrohydraulic lithotriptors, stainless steel or brass have been preferred. To analyze the effect of a new reflector material one may adjust the parameter in the simulation accordingly.

Nowadays, in the lithotriptors a water cushion is used to transmit the shock waves to the patient. Therefore, the selection of the outer medium as air makes sense. However, it is known that in an earlier version lithotripsy system (HM3, Dornier, Germany) the patient was placed in a tub and therefore the surrounding medium was water. In this model an extremely high performance has been achieved. The third test analyzed this phenomenon. In the simulation the points assigned as air was replaced with water and the value of the density was changed accordingly.

In Section 1 we mentioned that different size shock wave therapy systems are needed for various clinical applications. The fourth test investigated the feasibility of such a simulation environment in analyzing the effect of the reflector size to pressure distribution and maximum and minimum pressure levels in the focal zone. In this test we reduced the size of the reflector, and thus the focal point F2 moved 10.5 cm closer to the reflector.

Another important clinical issue in this field is the position of the shock wave generation electrode. It is reported by the clinicians that a shift in this position may be encountered in a clinical setup. The sparks formed between the tips of the

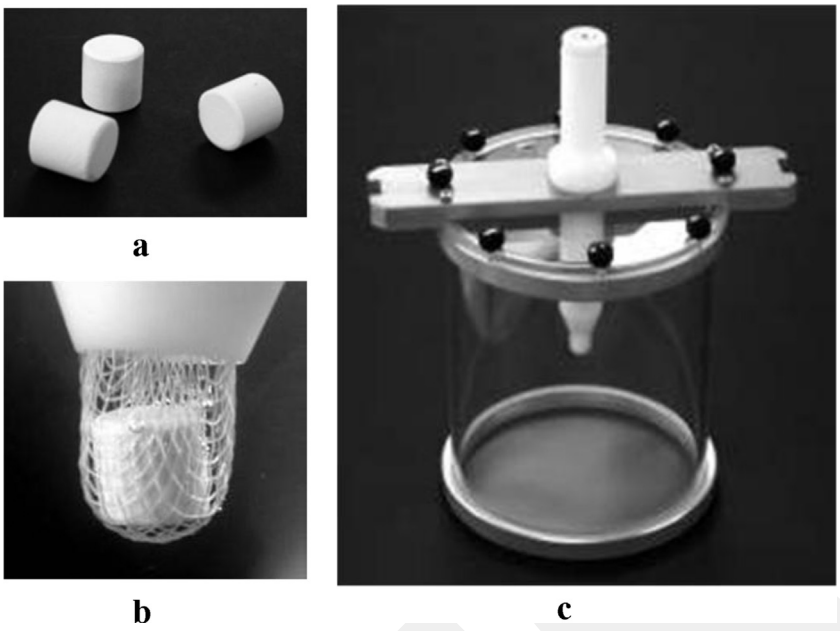

Fig. 3 – (a) Test stone, (b) test stone is placed on the F2 focal point, and (c) experimental apparatus to be attached to the lithotriptor head.

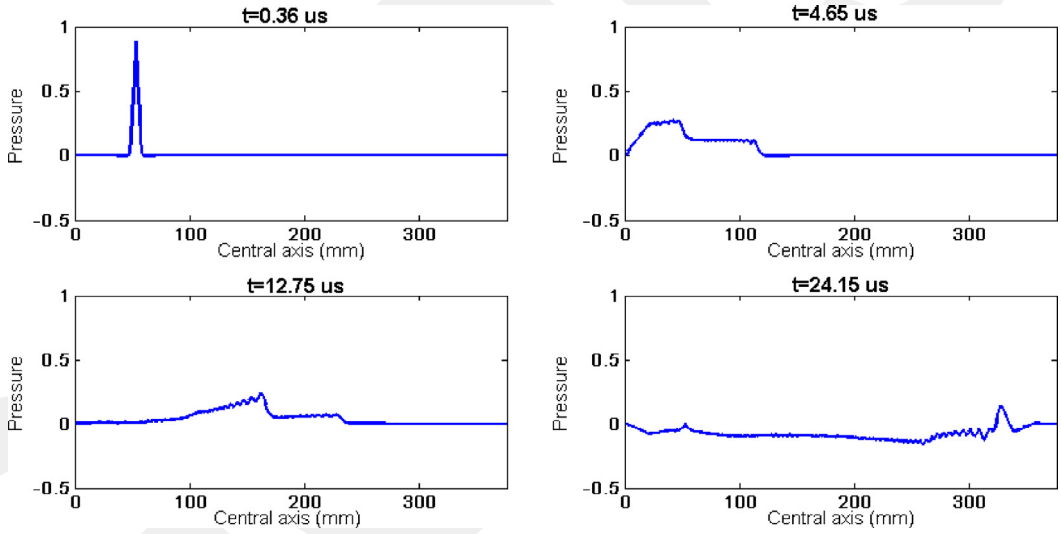

Fig. 4 – Normalized pressure values on the z-axis (central axis between F1 and F2 focal points) for four different instants of time.

electrode bring about deformation on the electrode tips because of the high temperature and pressure in that small region. The deformation increases the distance between the tips, which in turn results in a shifted focal source position. This causes a decrease in the focal zone pressure values. In the last test we analyzed this issue by shifting the shock wave source location to a point 5 mm right of F1 focal point.

3. Results

One of the most suitable ways to observe the maximum pressure point in the focal zone is to plot the graphs of pressure values on the z-axis corresponding to the line between the ellipsoid focal points F1 and F2. Fig. 4 shows the normalized pressure values on the z-axis for four different instants in time, from just after the onset of the shock wave at F1 point to the instant in which the maximum pressure value is reached in focal zone. These instants are selected in order to depict the propagation characteristics changing in time. As shown in Fig. 5, focusing on the proximity of F2 point demonstrates the fact that maximum pressure point (P^+ point) is shifted 4 mm further on the z-axis instead of being on the F2 point. In this figure, it is possible to observe that on the maximum pressure point the high negative pressure occur just before the high positive pressure reaches to that point, which induces a

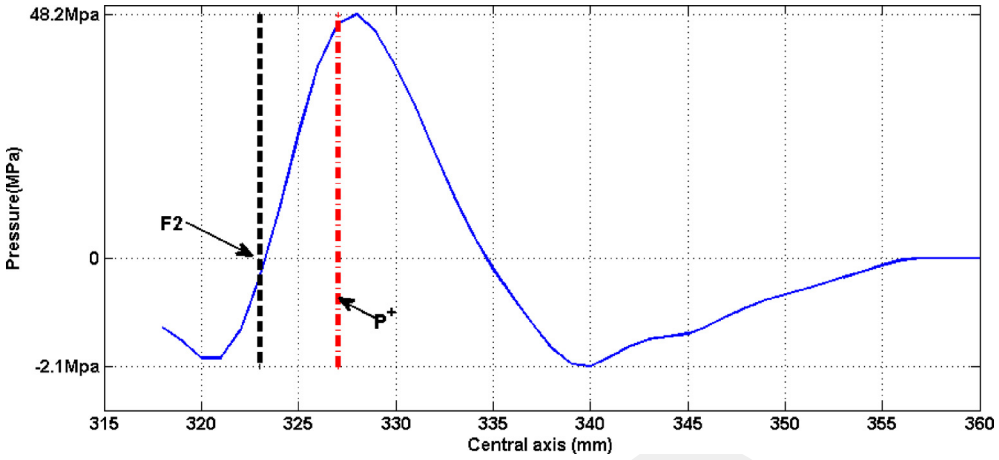

Fig. 5 – Zoomed graph showing the actual pressure values on the proximity of F2 point when the instant of time in the simulation was 24.15 μs. Black and red lines indicate the F2 and maximum pressure (P^+) points.

shear-stress on the stone. The shear-stress created due to the positive and negative pressures on the focal zone is known to be one of the mechanisms used to explain the disintegration of the stone.

Instead of demonstrating the results as 1D graphs, it is also informative to show the pressure distribution on the x–z plane where F1 and F2 points exist and the ellipsoid reflector is cut into two symmetric halves. In Fig. 6, the pressure distributions on the x–z plane for four different instants in time (same with the instants used in Fig. 4) are depicted. The reflection from the ellipsoid reflector and the focusing on the focal zone can easily be demonstrated using these graphs. The shear-stress effect is also obvious in the last graph showing the positive and negative pressure regions closely located in the focal zone. Figs. 5 and 6 include representative graphs which will be presented in the later parts of this section.

In the experiments with test stones, for the tap water with 2.5 mg of gas in 1 l water an average of 315 shocks for five test stones were used to totally disintegrate each stone, and, an average of 260 shocks for other five stones tested in 1.5 mg gas in 1 l water. This result showed that the effect of each shock on the stone increased when the amount of gas in water was decreased. For the first simulation test type, we observed that the maximum pressure value on the P^+ point rose from 48.200 to 48.260 MPa, and negative pressure value occurring approximately 12 mm from P^+ point decreased from −2.100 to −2.138 MPa. The absolute difference between positive and negative pressures increased ~0.1 MPa, which might affect the stone after certain number of shocks.

We observed in the simulations that increasing the temperature of the propagation medium from 0 to 30 °C mainly affected the total propagation duration needed to reach the focal zone. There was a 2 μs delay when the temperature was reduced. The general waveform did not change; however, negative pressure value occurring proximal to the F2 point was lower when the temperature was 30 °C. When aluminum was used instead of brass as the reflector material, the simulation results showed that the maximum positive pressure level diminished from 48.2 to 22.0 MPa, proving the fact that aluminum is not a good reflector. The simulation of HM3 model, in which the patient was placed in a tub filled with water, we observed incredibly high maximum pressure levels (up to 120 MPa). These high pressures in the focal zone were reached because the absorption of pressure waves by air was

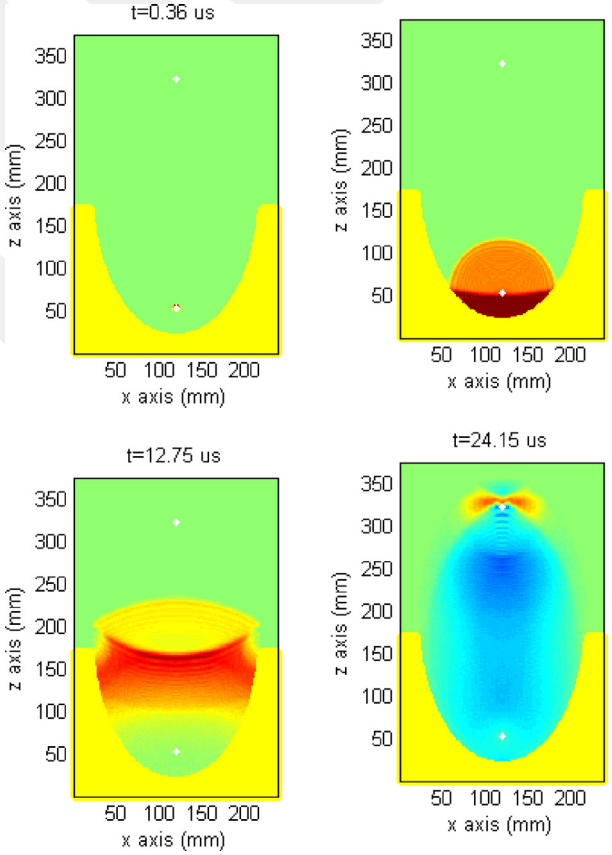

Fig. 6 – Pressure distribution on x–z plane for the time instants mentioned in Fig. 4. Red and blue show positive and negative pressure values, respectively. (For interpretation of the references to color in this figure legend, the reader is referred to the web version of this article.)

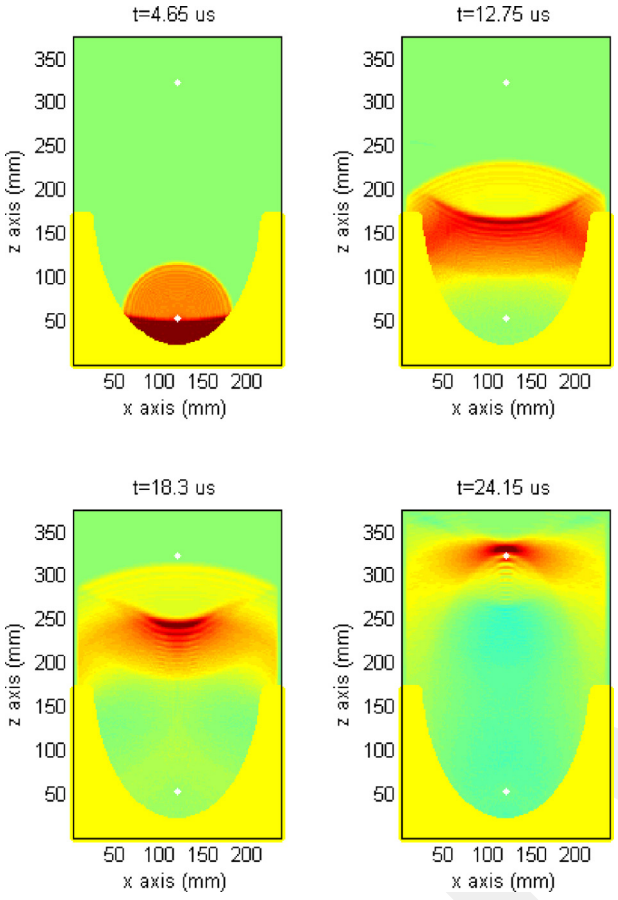

Fig. 7 – Pressure distribution on the *x–z* plane for four instants in time in the simulation when the outer medium (air) was replaced with water in the simulations. Maximum pressure level was 120 MPa.

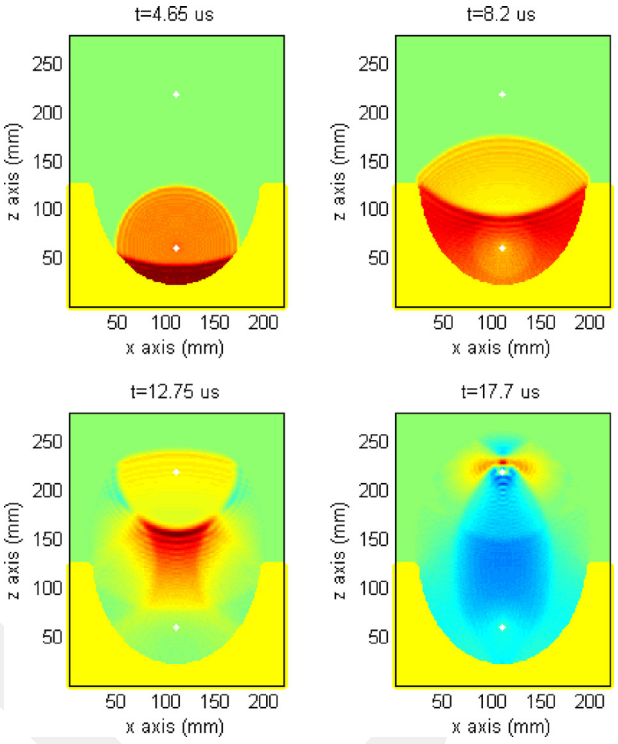

Fig. 8 – The effect of smaller reflector on the computed pressure levels for four different instants of time in the simulation.

eliminated. Fig. 7 depicts that high pressure values span a larger region on the focal zone.

The change in size of the reflector moved F2 point ~10.5 cm on the z-axis toward the reflector. The smaller size caused an increase in the computed maximum positive pressure (from 48.200 MPa to 73.340 MPa). This increase occurred due to shorter duration and distance for the shock wave to propagate to the focal zone and with less attenuation because of less absorption. Fig. 8 depicts the 2D distribution of pressure on x–z plane.

Finally, the simulation results showing the effect of focal source shift were quite interesting (see Fig. 9). The reflected waves could not be focussed on the focal zone, and thus, the pressure distribution on the zone was not as efficient as it was for a proper positioning of the focal source. The high pressures were obtained out of the focal zone.

4. Discussion

The main motivation for this study was to develop a general purpose numerical simulation environment by which three-dimensional ultrasonic shock wave propagation present in medical devices used in shock wave therapy can be investigated. In this simulation environment the parameters that may affect the performance can be adjusted manually and the results can be visualized in an effective manner. We tested our simulation program on a commercial lithotriptor and found that this is a feasible approach to investigate the effects of various design parameters and medium properties. Specifically, we constructed our realistic computational model using finite-difference time-domain approach and optimized the model using the experimental results obtained by the manufacturer. In addition, we qualitatively compared the simulation results with the experimental results from a test in which the gas amount in water was changed. Moreover, we investigated the effects of changes in various parameters to the performance of the electrohydraulic lithotripsy system.

The shock wave therapy systems are commonly used to break kidney stones into fragments. Nowadays, these systems are also used in certain orthopedic operations and several ongoing investigational studies for the treatment of cancer and cardiovascular diseases. Because of these new application areas we need novel shock wave therapy system designs for different kinds of treatment strategies. The best way to reduce design time and cost is to create a computational model of the system which would also give the designer flexibility while testing the effect of new parameters.

In this study we focused on the electrohydraulic lithotripsy systems because in order to validate the simulation results we only had experimental data from such a system. However, it is

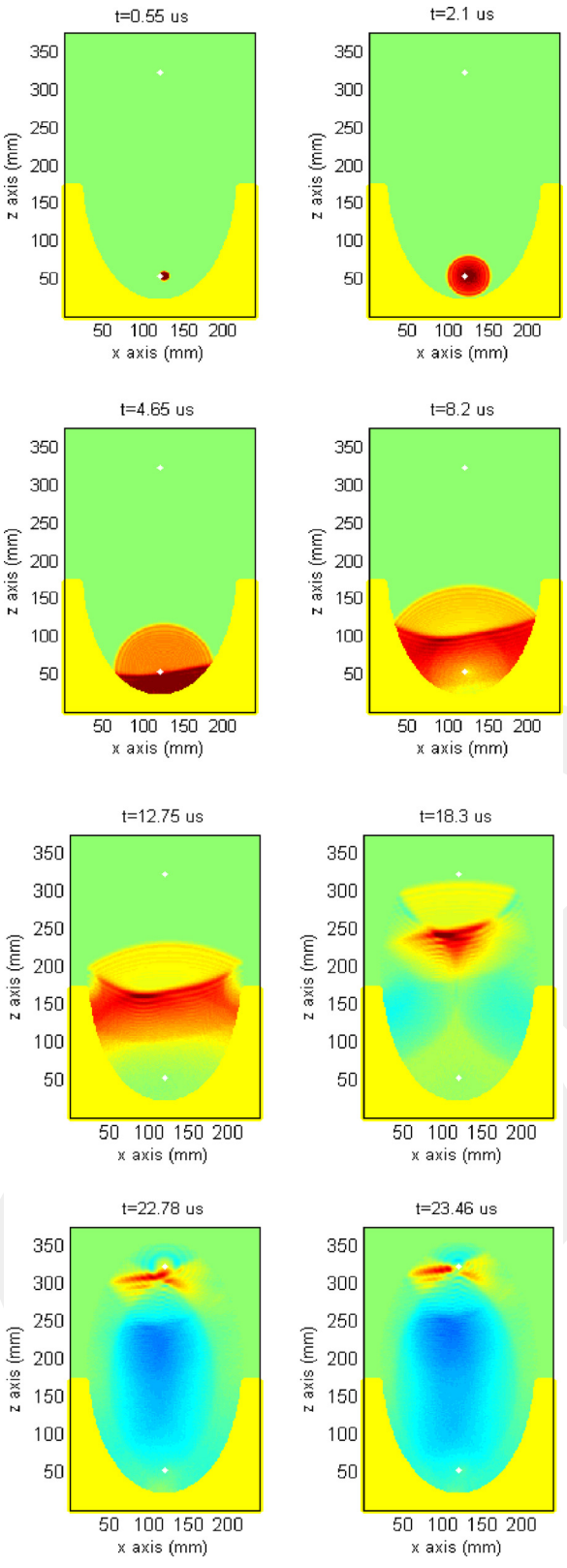

Fig. 9 – The simulation results showing the effect of focal source point shift for eight different instants in time.

also possible to modify the code for the implementation of a piezoelectric or an electromagnetic lithotriptor. In the piezoelectric lithotripsy systems, the pressure wave is formed by activating the piezoelectric crystals placed on a sphere-shaped source (similar to the reflector used in an electrohydraulic system). In the numerical simulations, instead of a point source positioned on the F1 source point as in the electrohydraulic lithotripsy, linear pressure wave sources are assigned on each crystal and the pressure wave is focused on the F2 point. Similarly, in the electromagnetic lithotripsy systems, the pressure wave is formed using a linear wave source and focused on the F2 point using an acoustical lens. It is also possible to incorporate this approach in the simulations using appropriate modifications in the code.

The results of the simulations showed, in general, that relatively small changes in the parameters lead to great performance improvement, which, in turn, indicates the possibility of novel shock wave therapy system designs with better performance levels than current systems have.

Limitation of this study include that the simulation geometry is large in current clinical systems and the discretization of the geometry results in high number of discrete points on which the numerical computations are performed. When the number of points is decreased the accuracy of the model is lost and when it is increased the computation time becomes unaffordable. On the other hand, temporal iteration step size needs to be small in order to capture the details occurring in short time durations. A similar optimization is required for this step size.

Moreover, the reference experimental results (pressure wave values for different situations on different positions) obtained by the manufacturer were limited in this study. Because it is an expensive procedure to perform such validation tests, the manufacturer performs them once. If there were more detailed experimental data the simulations would have been more accurate.

In this study, we did not include any tools to investigate the effects of the shock wave on the human body, such as kidney tissues. This kind of an improvement is possible by incorporating three dimensional computed tomography images into the simulation environment.

Because of shock wave, some parts of the unit wear out after treatment. Lithotripsy units have to be recalibrated and tested in periods like once a month or shorter which is defined in manufacturer's service manual. The wear out process was also not incorporated in our simulation environment.

In addition, in this model we did not include other ESWL unit problems like high volume noise level. These units can create more than 85 dB noise in normal treatment, therefore during the treatment both patient and device operator should wear earplugs. This protection method and the noise levels are also described in related standards of FDA and CE. In this model it is possible to enlarge the buffer layer and simulate the noise effects of the units. Changing the buffer layer acoustic parameter from air to an isolation material can also be a good approach for further studies. However, in our study we adjusted the buffer area acoustic parameter to air and the size of the area to minimum. The main reason of this assumption is to minimize the simulation time.

There are also some details and minor effects between real test procedure and our model. To simplify our model and to decrease simulation time we had to make some assumptions. These assumptions may reduce the shock wave performance in real life but they are critical in work performance and service purposes. We can list some assumptions made in our model:

- Shock wave electrodes have to be changed in every new patient. To change the electrode the operator have to drain the water inside the ellipsoid, change the electrode, fill the ellipsoid with water and drain the bubbles inside the cushion. Because of this process there are 2 or 3 holes inside the ellipsoid, whose locations and sizes depend on the manufacturer. We also ignored these holes in our simulations.
- In newer models of ESWL, between the test stone (or hydrophone pressure sensors) and ellipsoid there is a rubber cushion about 1 mm thick. Earlier models of ESWL, described as the gold standard in [15], did not have such a cushion. We ignored this rubber material in our simulations.
- Between the two poles of the electrodes that are used for shock wave source in F1 focal point, there is a thin conductive wire for electrical connection. We ignored this cable and placed a shock wave source in the center of the F1 focal point.
- This study investigates the pressure effects of shock wave in ESWL. Rather then the pressure effect for stone disintegration there is also other effects like cavitation bubble [15]. This effect can be seen with ultra-high speed cameras during the tests. Because of their random nature it is difficult to incorporate this fact into our model. We ignored this effect in our shock wave performance calculations.

These assumptions have minor effects to our simulation performance. We optimized our model with the experimental results obtained by manufacturer and our own results, and then studied the effects of various parameters.

Our future studies will include numerical simulations on a realistic patient geometry with fatty and kidney tissue and a stone on the F2 point incorporated to the simulation environment. By this way, it will be possible to investigate the effects of the shock wave therapy in an in vivo setup. In addition, we will also study the pressure wave simulations for the new devices used in the orthopedics and other applications.

Furthermore, the finite-element time-domain (FETD) approach may also be an alternative to the FDTD method, which is an ongoing effort in our laboratory.

The results of this study encourage further investigation and provide adequate evidence that the numerical modeling of a shock wave therapy system is feasible and can provide a practical means to test novel ideas in new device design procedures.

Conflict of interest

There is no conflict of interest.

Acknowledgment

We would like to thank Cengiz KABAKCI (The founder and the CEO of PCK Electronics Ltd, Ankara, Turkey) for providing us with the lithotripsy system manufacturer's experimental data.

REFERENCES

[1] H. Gollwitzer, P. Diehl, A. von Korff, V.W. Rahlfs, L. Gerdesmeyer, Extracorporeal shock wave therapy for chronic painful heel syndrome: a prospective, double blind, randomized trial assessing the efficacy of a new electromagnetic shock wave device, Journal of Foot and Ankle Surgery 46 (5) (2007) 348–357.
[2] R. Buchbinder, R. Ptasznik, J. Gordon, J. Buchanan, J. Prabaharan, A. Forbes, Ultrasound-guided extracorporeal shock wave therapy for plantar fasciitis: a randomized controlled trial, JAMA: The Journal of the American Medical Association 288 (2002) 1364–1372.
[3] B. Chung, J.P. Wiley, Effectiveness of extracorporeal shock wave therapy in the treatment of previously untreated lateral epicondylitis: a randomized controlled trial, American Journal of Sports Medicine 32 (2004) 1660–1667.
[4] T. Uwatoku, K. Ito, K. Abe, K. Oi, T. Hizume, K. Sunagawa, H. Shimokawa, Extracorporeal cardiac shock wave therapy improves left ventricular remodeling after acute myocardial infarction in pigs, Coronary Artery Disease 8 (5) (2007) 397–404.
[5] N. Takahiro, H. Shimokawa, K. Oi, H. Tatewaki, T. Uwatoku, K. Abe, et al., Extracorporeal cardiac shock wave therapy markedly ameliorates ischemia induced myocardial dysfunction in pigs in vivo, Circulation 110 (2004) 3055–3061.
[6] R. Canaparo, L. Serpe, M.G. Catalano, O. Bosco, G.P. Zara, L. Berta, R. Frairia, High energy shock waves (HESW) for sonodynamic therapy: effects on HT-29 human colon cancer cells, Anticancer Research 26 (5A) (2006) 3337–3342.
[7] K. Yee, Numerical solution of initial boundary value problems involving Maxwell's equations in isotropic media, IEEE Transactions on Antennas and Propagation 14 (1966) 302–307.
[8] A. Taflove, Computational Electrodynamics: The Finite Difference Time Domain Method, Artech House, Boston, 1995.
[9] E. Steiger, FD-TD-modeling of propagation of high energy sound pulses in lithotripter-tissue-arrangements, in: Proc. IEEE Int. Ultrasonics Symp., Toronto, Canada, October 5–8, 1997.
[10] X.Q. Jian, N. Morita, Q.D. Shi, O. Nakamura, D.S.H. Liu, FDTD simulation of nonlinear ultrasonic pulse propagation in ESWL, in: Proc. of IEEE Eng. in Med. and Biol, 27th Annual Conference, Shanghai, China, 2005.
[11] H. Reichenberger, Lithotripter systems, Proceedings of the IEEE 76 (1988) 1236–1246.
[12] Y. Ukai, S. Ishidaa, N. Hataa, T. Azumab, S. Umemurab, T. Dohia, A 3-D simulation of focused ultrasound propagation for extracorporeal shock wave osteotomy, in: Proc. 17th Int. Congress and Exhibition, Computer Assisted Radiology and Surgery, 2003, pp. 658–663.
[13] D.M. Sullivan, Electromagnetic Simulation Using the FDTD Method, IEEE Press, New York, 2000.
[14] J.P. Berenger, A perfectly matched layer for the absorption of electromagnetic waves, Journal of Computational Physics 114 (2) (1994) 185–200.
[15] J.J. Rassweiler, G.G. Tailly, C. Chaussy, Progress in Lithotriptor Technology, EAU Update Series 3 (1) (2005) 17–36.